

Electronic Supplementary Information (ESI)

Highly luminescent near-infrared Cu-doped InP quantum dots with Zn–Cu–In–S/ZnS double shell scheme

Jiyong Kim,^a Hyung Seok Choi,^a Armin Wedel,^a Suk-Young Yoon,^b Jung-Ho Jo,^b Hyun-Min Kim,^b Chul-Jong Han,^c Hong-Joo Song,^c Jeong-Min Yi,^c Jong-Shik Jang,^d Hannes Zschiesche,^e Bum-Joo Lee,^{*f} Kyoungwon Park^{*c} and Heesun Yang^{*b}

^a Functional Materials and Devices, Fraunhofer Institute for Applied Polymer Research, Potsdam 14476, Germany

^b Department of Materials Science and Engineering, Hongik University, Seoul 04066, Korea

^c Display Research Center, Korea Electronics Technology Institute, Seongnam-si, Gyeonggi-do 05658, Korea

^d Analytical Instrumentation Center, Industry-University Cooperation Foundation, Hanyang University, Seoul 04763, Korea

^e Department of Colloid Chemistry, Max Planck Institute of Colloids and Interfaces, Potsdam 14476, Germany

^f Graduate School of Flexible and Printable Electronics, Jeonbuk National University, Jeonju, Jeollabuk-do 54896, Korea

Table S1 Absolute PL QYs of InP:Cu QDs synthesized from Cu²⁺ and Cu⁺ with/without DDT.

QD	Absolute PL QY (%)			
	Cu ²⁺ (with DDT)	Cu ²⁺	Cu ⁺ (with DDT)	Cu ⁺
InP:Cu	26.7	12.2	21.5	9.4

Table S2 Absolute PL QYs of InP, InP:Cu, InP:Cu/ZCIS, and InP:Cu/ZCIS/ZnS QDs produced from different-sized InP cores used for Cu doping.

QD	Absolute PL QY (%)			
	532 nm (QD1)	567 nm (QD2)	610 nm (QD3)	632 nm (QD4)
InP	7.5	13.2	12.1	10.5
InP:Cu	20.5	26.7	25.5	24.8
InP:Cu/ZCIS	60.8	64.8	61.5	60.4
InP:Cu/ZCIS/ZnS	72.7	82.4	73.3	71.5

Table S3 ICP-OES results of QDs for each synthetic step.

QD	Element			
	In ^P	S ^P	Zn ^P	Cu ^P
InP:Cu	1.23	0.34	0.73	0.5
InP:Cu/ZCIS	4.65	3.07	1.89	0.72
InP:Cu/ZCIS/ZnS	3.23	7.92	9.36	0.65

P = the mole ratio calculated based on phosphine atom

Table S4 TEM-EDS-based elemental composition results on InP:Cu/ZCIS/ZnS QDs.

QD	Concentration (atomic %)				
	In	S	Zn	Cu	P
InP:Cu/ZCIS/ZnS	12.5	27.8	39.3	2.5	3.6

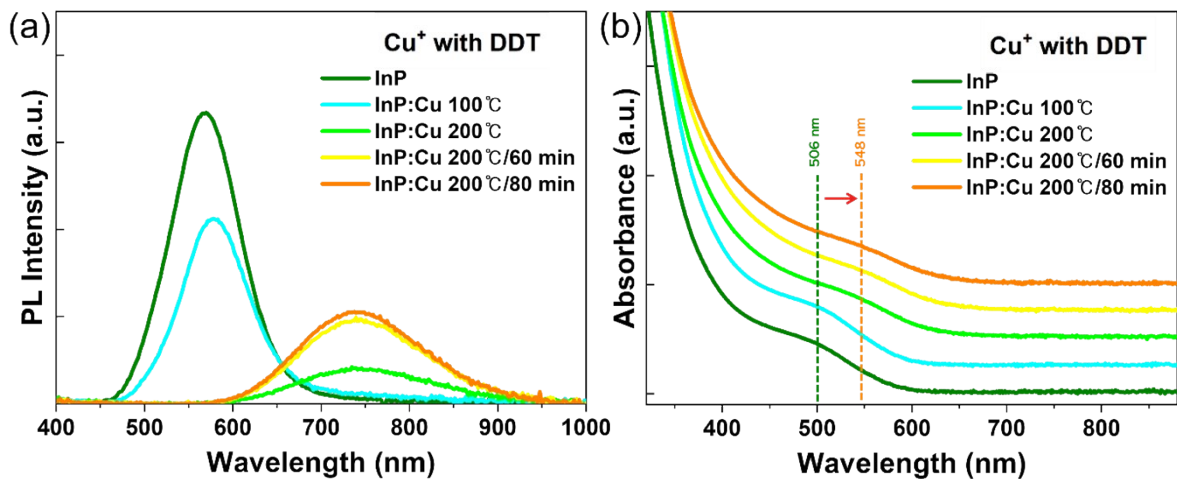


Fig. S1 (a) PL and (b) absorption spectral evolutions with different synthetic temperatures and annealing times when Cu doping was performed by using CuCl with DDT. Vertical dotted lines in (b) show the red-shift of 1S peaks from initial InP to final InP:Cu QDs.

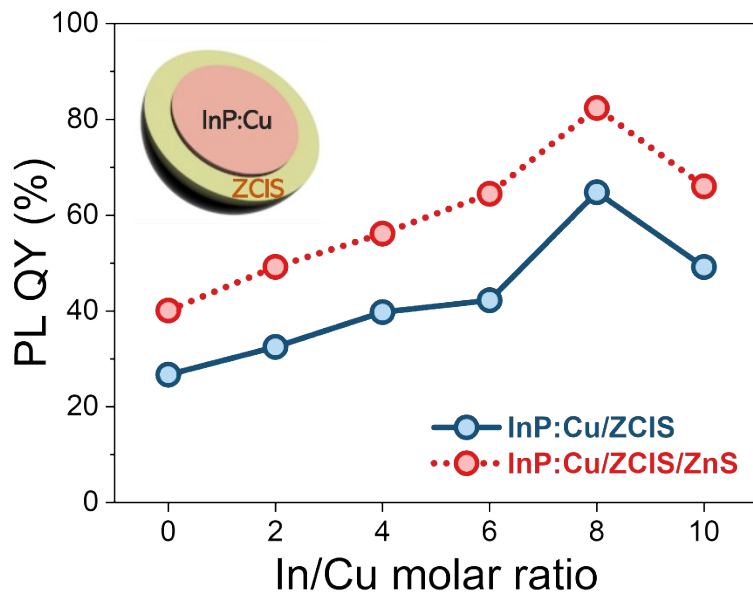


Fig. S2 Changes of PL QY of InP:Cu/ZCIS and InP:Cu/ZCIS/ZnS QDs as a function of nominal In/Cu molar ratio used in ZCIS shelling step.

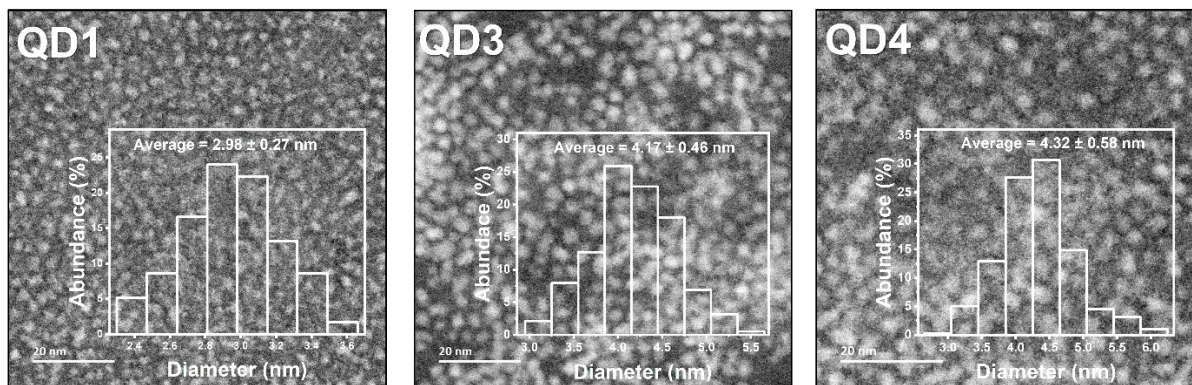


Fig. S3 Annular dark-field scanning transmission electron microscopy (ADF-STEM) images and size histograms of QD1 (532 nm), QD3 (610 nm), and QD4 (628 nm), showing average sizes of 2.98 ± 0.27 , 4.17 ± 0.46 , and 4.32 ± 0.58 nm, respectively.

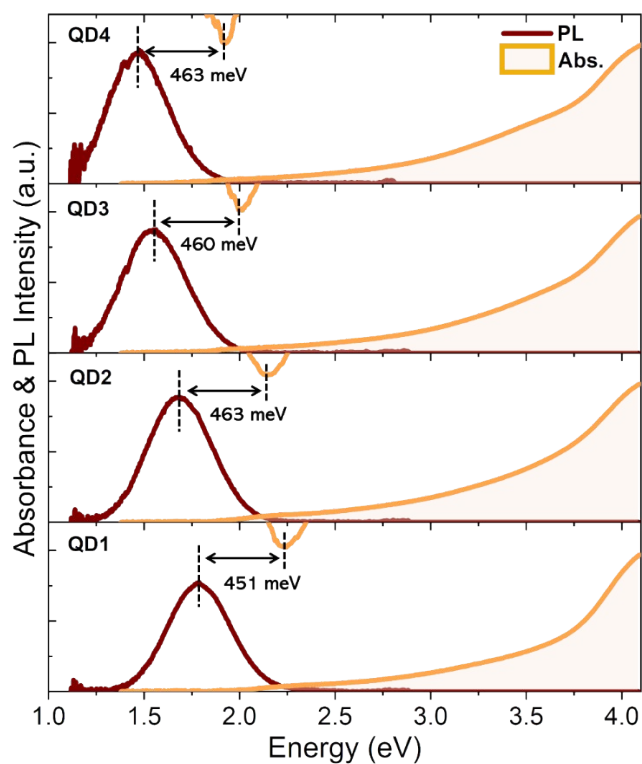


Fig. S4 PL versus original and its second derivative absorption spectra of a series of InP:Cu/ZCIS/ZnS QDs synthesized from QD1–4, resulting in overall large Stokes shifts of 451–463 meV.

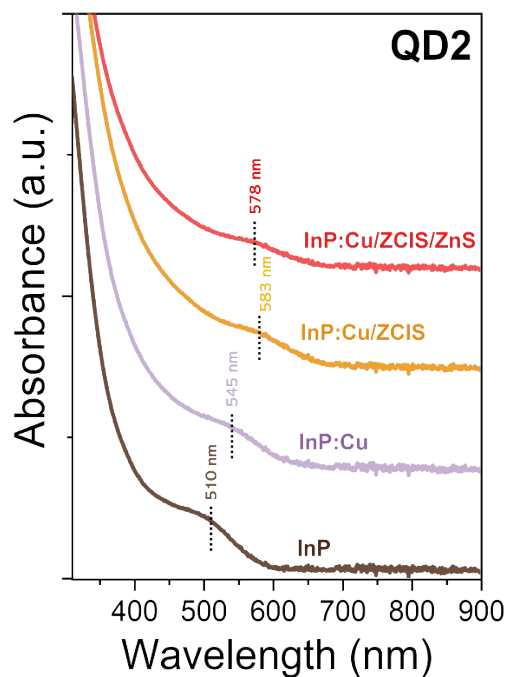


Fig. S5 Absorption spectra of InP, InP:Cu, InP:Cu/ZCIS, and InP:Cu/ZCIS/ZnS QDs, showing a slight blue-shift from InP:Cu/ZCIS (583 nm) to InP:Cu/ZCIS/ZnS QDs (578 nm).

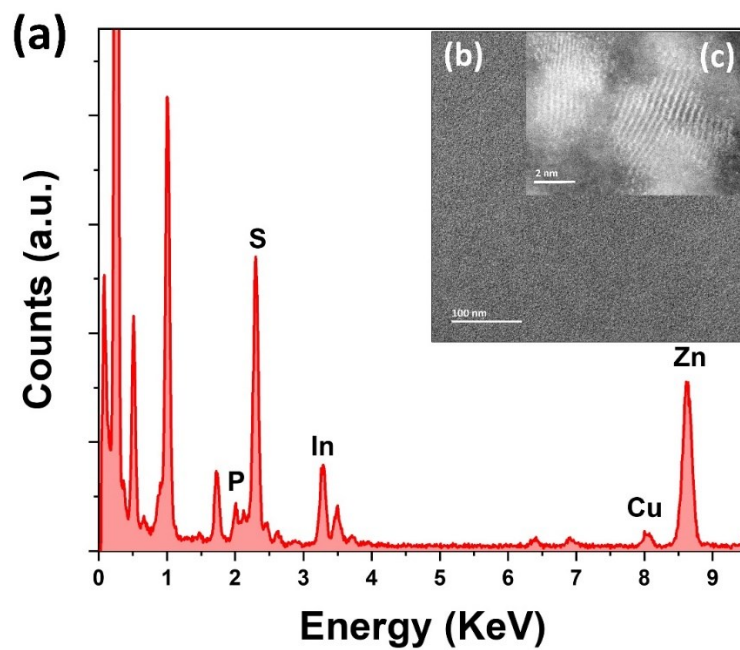


Fig. S6 (a) EDS spectrum of InP:Cu/ZnS QDs acquired in (b) TEM image averaged over the broad area, and (c) STEM-ADF image of InP:Cu/ZnS QDs in one spot of (b).